RENORMALISATION EFFECTS OF NEUTRINO MASSES AND INTERACTIONS*

Smaragda Lola

CERN Theory Division
Geneva 23, CH-1211, Switzerland

(Received April 24, 2000)

We discuss neutrino thresholds in the light of the recent experimental data, which indicates the presence of neutrino oscillations. In particular, we analyse the effects of radiative corrections on the stability of neutrino textures and discuss how Yukawa unification is also affected. Renormalisation induced lepton flavour violating processes from non-zero neutrino masses are also studied.

PACS numbers: 14.60.Pq, 12.15.Ff, 12.60.–i, 11.10.Hi

1. Neutrino data and implications

The recent SuperKamiokande data [1] clearly indicates a ν_μ/ν_e ratio in the atmosphere that is significantly smaller than the theoretical expectations. The most natural way to explain this deviation, is by introducing ν_μ–ν_τ oscillations, with $\delta m^2_{\nu_\mu\nu_\tau} \approx (10^{-2}$ to $10^{-3})$ eV^2 and $\sin^2 2\theta_{\mu\tau} \geq 0.85$. Alternative schemes with dominant $\nu_\mu \to \nu_e$ oscillations are excluded by both the SuperKamiokande data on electron-like events [1], as well as by the data from the Chooz reactor experiment [2]. Finally, oscillations involving a sterile neutrino are disfavoured (but not yet excluded) by the azimuthal-angle dependence of muon-like events [1] and by measurements of π^0 production.

Once neutrino oscillations are introduced in order to explain the atmospheric neutrino deficit, it is natural to address similarly the solar neutrino puzzle. The latter can be resolved through either vacuum or matter-enhanced (MSW) oscillations. The first require a mass splitting of the neutrinos that are involved in the oscillations in the range $\delta m^2_{\nu_e\nu_\alpha} \sim (0.5$–$1.1) \times 10^{-10}$ eV^2, where α is μ or τ. MSW oscillations [3], on the other hand,

* Presented at the Cracow Epiphany Conference on Neutrinos in Physics and Astrophysics, Cracow, Poland, January 6–9, 2000.

require $\delta m^2_{\nu_e \nu_\alpha} \sim (0.3\text{–}20) \times 10^{-5}$ eV^2 with either large $\sin^2 2\theta_{e\alpha} \sim 1$ or small $\sin^2 2\theta_{e\alpha} \sim 10^{-2}$.

The implications of these observations are very interesting, since they point towards a non-zero neutrino mass and lepton-number violation, that is *the existence of physics beyond the standard model.* It turns out that both the solar and atmospheric neutrino data can be accommodated in a natural way in schemes with three light neutrinos with at least one large mixing angle and hierarchical masses, of the order of the required mass differences: $m_3 \sim (10^{-1}$ to $10^{-1.5})$ eV and $m_2 \sim (10^{-2}$ to $10^{-3})$ eV $\gg m_3$. On the other hand, if neutrinos are also to provide a significant hot dark matter component, three almost-degenerate neutrinos with masses of ≈ 1 eV would be required.

Along these lines, a natural question that arises is why neutrino masses are smaller that the rest of the fermion masses in the theory. This can be explained by the see-saw mechanism [4], which involves Dirac neutrino masses m^D_ν, of the same order as the charged-lepton and quark masses, and heavy Majorana masses $M_{\nu_{\rm R}}$ for the right-handed neutrinos, $\nu_{\rm R}$, in a way that light effective neutrino mass matrices at a scale M_N, such that:

$$m_{\rm eff} = m^D_\nu (M_{\nu_{\rm R}})^{-1} m^{D^T}_\nu \,. \tag{1}$$

For instance, for $m^D_\nu \approx 200$ GeV and $M_N \approx \mathcal{O}(10^{13}$ GeV), $m_{\rm eff} \approx 1$ eV. Then, in complete analogy to the quark currents, the leptonic mixing matrix is [5]

$$V_{\rm MNS} = V_\ell V^\dagger_\nu \,, \tag{2}$$

where V_ℓ diagonalizes the charged-lepton mass matrix, while V_ν diagonalizes the light neutrino mass matrix $m_{\rm eff}$.

In the presence of neutrino masses, the running of the various couplings from the unification scale down to low energies is modified. From $M_{\rm GUT}$ to M_N, one must include radiative corrections from the neutrino Yukawa couplings, while below M_N, the right-handed neutrinos decouple from the spectrum and an effective see-saw mechanism is operative. It actually turns out, as we are going to discuss in subsequent sections, that the renormalisation group effects give important information on the structure of the neutrino textures, while unification can also be affected by neutrino thresholds.

Neutrino oscillations involve violations of the individual lepton numbers $L_{e,\mu,\tau}$, raising the prospect that there might also exist observable processes that violate charged-lepton number conservation [6, 7], such as $\mu \to e\gamma$, $3e$ and $\tau \to \mu\gamma, 3\mu/e$, and $\mu \to e$ conversion on heavy nuclei [7–9]. In non-supersymmetric models with massive neutrinos, the amplitudes for the charged-lepton-flavour violation are proportional to inverse powers of the

right-handed neutrino mass scale $M_{\nu_{\rm R}}$ and thus the rates for rare decays are extremely suppressed [6]. On the other hand, in supersymmetric models these processes are only suppressed by inverse powers of the supersymmetry breaking scale, which is at most 1 TeV [7]. The present experimental upper limits on the most interesting of these decays are

$$\begin{aligned}
{\rm BR}(\mu \to e\gamma) &< 1.2 \times 10^{-11} \;:\; [10]\,, &(3)\\
{\rm BR}(\mu^+ \to e^+e^+e^-) &< 1.0 \times 10^{-12} \;:\; [11]\,, &(4)\\
{\rm R}(\mu^- Ti \to e^- Ti) &< 6.1 \times 10^{-13} \;:\; [12]\,, &(5)\\
{\rm BR}(\tau \to \mu\gamma) &< 1.1 \times 10^{-6} \;:\; [13]\,, &(6)
\end{aligned}$$

however, projects are currently underway to improve these upper limits significantly, especially in intense μ sources that might enable especially the upper limits on $\mu \to e$ transitions to be improved by several further orders of magnitude [14]. This indicates that it is of fundamental importance to understand the magnitude of the effects that one might expect, in association with neutrino oscillations.

2. Neutrino threshold effects

As we have already mentioned in the introduction, the running of couplings from the unification scale, $M_{\rm GUT}$, to low energies is modified by neutrino thresholds. The Dirac neutrino Yukawa coupling, λ_N, runs until the scale M_N. Subsequently it decouples and the quantity that runs is the effective neutrino operator $m_{\rm eff}$.

In order to understand the renormalization effects due to a non-zero λ_N between $M_{\rm GUT}$ and M_N, it is easier to start with the small-tan β regime of a supersymmetric theory where only the top and the Dirac neutrino Yukawa couplings contribute in a relevant way. The effect of the neutrino coupling to gauge unification is smaller than on the Yukawa ones, since it is only at two loop that λ_N enters in the running of α_i. In a diagonal basis [15], the renormalisation group equations of the Yukawa couplings take the following form:

$$\begin{aligned}
16\pi^2 \frac{d}{dt}\lambda_t &= \left(6\lambda_t^2 + \lambda_N^2 - G_U\right)\lambda_t\,,\\
16\pi^2 \frac{d}{dt}\lambda_N &= \left(4\lambda_N^2 + 3\lambda_t^2 - G_N\right)\lambda_N\,,\\
16\pi^2 \frac{d}{dt}\lambda_b &= \left(\lambda_t^2 - G_D\right)\lambda_b\,,\\
16\pi^2 \frac{d}{dt}\lambda_\tau &= \left(\lambda_N^2 - G_E\right)\lambda_\tau\,, &(7)
\end{aligned}$$

where $\lambda_\alpha : \alpha = t, b, \tau, N$, represent the third-generation Dirac Yukawa couplings for the up and down quarks, charged lepton and neutrinos, respectively, and the $G_\alpha \equiv \sum_{i=1}^{3} c_\alpha^i g_i(t)^2$ are functions that depend on the gauge couplings, with the coefficients c_α^i given in [15]. In terms of the various Yukawa couplings λ_{t_0}, λ_{N_0},λ_{b_0}, λ_{τ_0}, at the unification scale, we can derive simple expressions which indicate how neutrinos affect the rest of the Yukawa couplings of the theory. Indeed [16]:

$$\lambda_t(t) = \gamma_U(t)\lambda_{t_0}\xi_t^6\xi_N\,, \qquad \lambda_N(t) = \gamma_N(t)\lambda_{t_0}\xi_t^3\xi_N^4\,, \tag{8}$$

$$\lambda_b(t) = \gamma_D(t)\lambda_{b_0}\xi_t\,, \qquad \lambda_\tau(t) = \gamma_E(t)\lambda_{\tau_0}\xi_N\,, \tag{9}$$

$$\gamma_\alpha(t) = \exp\left(\frac{1}{16\pi^2}\int_{t_0}^{t} G_\alpha(t)\,dt\right) = \prod_{j=1}^{3}\left(\frac{\alpha_{j,0}}{\alpha_j}\right)^{c_\alpha^j/2b_j}\,, \tag{10}$$

$$\xi_i = \exp\left(\frac{1}{16\pi^2}\int_{t_0}^{t}\lambda_i^2\,dt\right)\,. \tag{11}$$

As noted, these results are valid for small $\tan\beta$. For large $\tan\beta$, the bottom and tau Yukawa couplings start playing an important role and the complete form of the renormalisation group equations is given in [17].

Below the right-handed Majorana mass scale, where $m_{\rm eff}$ is formed, λ_N decouples from the renormalisation group equations. However, the effective neutrino mass operator will be a running quantity. For a generic $\tan\beta$

$$\frac{1}{m_{\rm eff}^{ij}}\frac{d}{dt}m_{\rm eff}^{ij} = \frac{1}{8\pi^2}\left(-c_i g_i^2 + 3\lambda_t^2 + \frac{1}{2}(\lambda_i^2+\lambda_j^2)\right)\,, \tag{12}$$

where i, j are lepton flavour indices, already indicating that large Yukawa terms, which lower the effective couplings, have a larger effect on $m_{\rm eff}^{33}$ than on the other entries. Finally, the neutrino mixing angle relevant for the atmospheric neutrino deficit, θ_{23}, is also a running quantity, given by [18,19]

$$16\pi^2\frac{d}{dt}\sin^2 2\theta_{23} = 2\sin^2 2\theta_{23}(1-2\sin^2\theta_{23})(\lambda_\tau^2-\lambda_\mu^2)\,\frac{m_{\rm eff}^{33}+m_{\rm eff}^{22}}{m_{\rm eff}^{33}-m_{\rm eff}^{22}}\,, \tag{13}$$

where the initial conditions for the running from M_N down to low energies are determined by the running of couplings between $M_{\rm GUT}$ and M_N.

3. Renormalisation of the neutrino mass operator and stability properties of neutrino textures

From equation (12), we already see that the neutrino masses will in fact vary non-trivially with the energy. Given the very small mass differences that one requires for solutions to the solar and the atmospheric neutrino deficits, it is natural to wonder whether a SuperKamiokande friendly texture at the GUT scale is still a solution at low energies.

It is convenient for the subsequent discussion to define the integrals

$$I_g = \exp\left[\frac{1}{8\pi^2}\int_{t_0}^{t}(-c_i g_i^2 dt)\right], \tag{14}$$

$$I_t = \exp\left[\frac{1}{8\pi^2}\int_{t_0}^{t}\lambda_t^2 dt\right], \tag{15}$$

$$I_i = \exp\left[\frac{1}{8\pi^2}\int_{t_0}^{t}\lambda_i^2 dt\right], \quad i=e,\mu,\tau\,. \tag{16}$$

Simple integration of (12) yields

$$\begin{aligned}\frac{m_{\rm eff}^{ij}}{m_{\rm eff,0}^{ij}} &= \exp\left\{\frac{1}{8\pi^2}\int_{t_0}^{t}\left(-c_i g_i^2 + 3\lambda_t^2 + \frac{1}{2}(\lambda_i^2+\lambda_j^2)\right)\right\}, \\ &= I_g\cdot I_t\cdot\sqrt{I_i}\cdot\sqrt{I_j}\,,\end{aligned} \tag{17}$$

where the initial conditions are denoted by $m_{\rm eff,0}^{ij}$. As we have already noted, these conditions are defined at M_N, the scale where the neutrino Dirac coupling λ_N decouples from the renormalisation-group equations.

Using (17), we see that an initial texture $m_{\rm eff,0}^{ij}$ at M_N is modified to become [20].

$$m_{\rm eff} \propto \begin{pmatrix} m_{\rm eff,0}^{11}\, I_e & m_{\rm eff,0}^{12}\,\sqrt{I_\mu}\,\sqrt{I_e} & m_{\rm eff,0}^{13}\,\sqrt{I_e}\,\sqrt{I_\tau} \\ m_{\rm eff,0}^{21}\,\sqrt{I_\mu}\,\sqrt{I_e} & m_{\rm eff,0}^{22}\, I_\mu & m_{\rm eff,0}^{23}\,\sqrt{I_\mu}\,\sqrt{I_\tau} \\ m_{\rm eff,0}^{31}\,\sqrt{I_e}\,\sqrt{I_\tau} & m_{\rm eff,0}^{32}\,\sqrt{I_\mu}\,\sqrt{I_\tau} & m_{\rm eff,0}^{33}\, I_\tau \end{pmatrix} \tag{18}$$

at $m_{\rm SUSY}$ [1].

[1] For small $\tan\beta$, ignoring at a first approximation all the Yukawa couplings except the top one, an initial texture $m_{\rm eff}(M_N)^{ij}$ at M_N becomes at a lower scale $m_{\rm eff} \propto I_g\cdot I_t\cdot m_{\rm eff}(M_N)$.

Even before performing a complete numerical analysis, we can make several observations:

- We first note that the relative structure of $m_{\rm eff}$ is only modified by the charged-lepton Yukawa couplings. On the contrary, the top and gauge couplings give only an overall scaling factor.

- Because of the factorization in (18), although the individual masses and mixings get modified, any mass matrix which is singular with a vanishing determinant — leading to a zero mass eigenvalue — remains so at the one-loop level.

- The Yukawa renormalization factors I_i are less than unity, and lead to the mass ordering $m_{\nu_e} > m_{\nu_\mu} > m_{\nu_\tau}$, if we start with exactly degenerate neutrinos at $M_{\rm GUT}$.

- For values of $I_{\tau,\mu}$ different from unity, the renormalization effects can be significant even for the light-generation sector, since, very small mass differences are required for addressing the solar neutrino problem.

In order to quantify the renormalization effects on the physical neutrino masses, we start with a texture which at the GUT scale leads to three *exactly degenerate* neutrinos, with scaled eigenvalues 1, -1, 1 and calculate the respective values at low energies [20]. We take as illustrative initial conditions $\alpha_{\rm GUT}^{-1} = 25.64$, $M_{\rm GUT} = 1.1 \times 10^{16}$ GeV and $m_{\rm SUSY} = 1$ TeV. We also choose λ_b/λ_τ such that an intermediate scale $M_N = 10^{13}$ GeV is consistent with the observed pattern of fermion masses The values of I_τ and I_μ that we find with these inputs are given in the first three columns of Table I and can be used to estimate the effects on the neutrino eigenvalues, mixings and mass differences in the specific texture with three exactly degenerate neutrinos, as shown in the last three columns of Table I, and in Fig. 1.

TABLE I

Values of I_τ and I_μ, for $M_N = 10^{13}$ GeV and different choices of λ_τ. Also tabulated are the three renormalized mass eigenvalues calculated for three exactly degenerate neutrinos for the unrenormalised texture.

λ_τ	I_τ	I_μ	m_3	m_2	m_1
3.0	0.826	0.9955	0.866	−0.952	0.997
1.2	0.873	0.9981	0.903	−0.966	0.998
0.48	0.9497	0.9994	0.962	−0.987	0.9996
0.10	0.997	0.99997	0.9478	−0.9993	0.99998
0.013	0.99997	1.00000	0.99998	−0.99999	1.00000

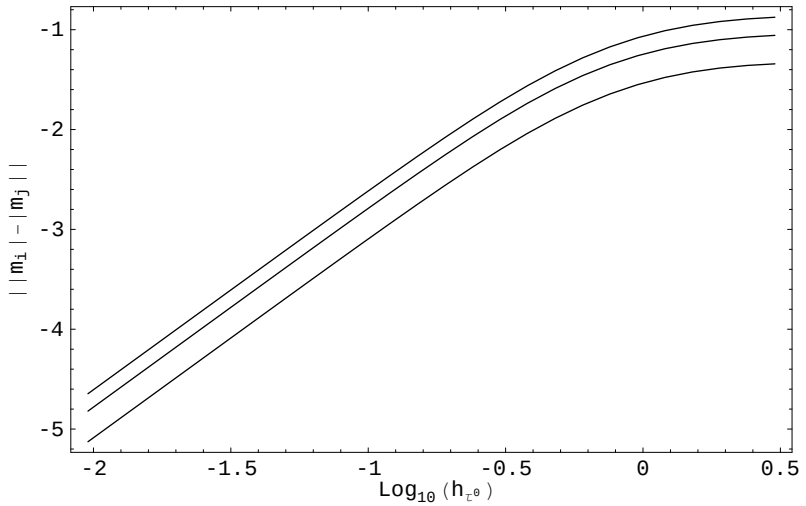

Fig. 1. Renormalization of $m_{\rm eff}$ eigenvalues for different initial values of λ_τ corresponding to values of $\tan\beta$ in the range 1 to 58, assuming three exactly degenerate neutrinos and $M_N = 10^{13}$ GeV. We see that the vacuum-oscillation scenario is never accommodated.

We see that the renormalization-group effects on the neutrino-mass eigenvalues are significant and spoil the neutrino degeneracy. It is apparent from Table I and Fig. 1 that the breaking of the neutrino-mass degeneracy in this model is unacceptable even for small $\tan\beta$. However, we should note that methods to stabilise the neutrino textures have been proposed. For instance, one can have textures that due to a symmetry are already non-degenerate at the high scales of the theory, [21]. Moreover, it may be that the structure of the Dirac neutrino mass matrices stabilises the textures [22].

Moreover, as indicated by Eq. (13), even the mixing angle may significantly change from the GUT scale to low energies *(i)* if λ_τ is large, and *(ii)* if the diagonal entries of $m_{\rm eff}$ are close in magnitude. To quantify this statement analytically, we may integrate the differential equations for the diagonal elements of the effective neutrino mass matrix [19], yielding the result

$$\frac{m^{33}_{\rm eff} + m^{22}_{\rm eff}}{m^{33}_{\rm eff} - m^{22}_{\rm eff}} = \frac{m^{33}_{\rm eff,0} I_\tau + m^{22}_{\rm eff,0}}{m^{33}_{\rm eff,0} I_\tau - m^{22}_{\rm eff,0}} \equiv f(I_\tau)\,.$$

Because of the running of the τ Yukawa coupling being larger than those for the other flavours of charged leptons, $m^{33}_{\rm eff}$ decreases more rapidly than $m^{22}_{\rm eff}$. Then if one starts with $m^{22}_{\rm eff} < m^{33}_{\rm eff}$ but both still relatively close in magnitude, for a sufficiently large I_τ, at a given scale we obtain $m^{22}_{\rm eff} = m^{33}_{\rm eff}$

and the mixing angle becomes *maximal*. The larger λ_τ^0, the earlier the entries may become equal. The exact scale where the mixing angle is maximal is given by the relation

$$I_\tau = \frac{m^{22}_{\text{eff},0}}{m^{33}_{\text{eff},0}}\,. \tag{19}$$

After reaching the maximal angle at some intermediate scale, the running of λ_τ results in $m^{33}_{\text{eff},0} < m^{22}_{\text{eff},0}$, changing the sign of $f(I_\tau)$ and thus resulting in a decrease of the mixing. In order, therefore, for a texture of this type to be viable, there needs to be a balance between the magnitudes of λ_τ and $m^{33}_{\text{eff}} - m^{22}_{\text{eff}}$ at the GUT scale [2].

Moreover, there might be additional intrinsic instabilities on the neutrino mixing. To see this, let us discuss the renormalization of the neutrino mixing angles, considering a perturbation ε from a texture that for $\varepsilon = 0$ leads to three exactly degenerate neutrinos:

$$m'_{\text{eff}} \propto \begin{pmatrix} 0 & \frac{1}{\sqrt{2}} & \frac{1}{\sqrt{2}}(1+\frac{\varepsilon}{2}) \\ \frac{1}{\sqrt{2}} & \frac{1}{2} & -\frac{1}{2}(1+\frac{\varepsilon}{2}) \\ \frac{1}{\sqrt{2}}(1+\frac{\varepsilon}{2}) & -\frac{1}{2}(1+\frac{\varepsilon}{2}) & \frac{1}{2}(1+\varepsilon) \end{pmatrix}. \tag{20}$$

Here, ε is a small quantity, which might arise from renormalisation group running or from some other higher-order effects such as higher-dimensional non-renormalizable operators. This perturbation lifts the degeneracy of the eigenvalues, which are now given by

$$1, \quad -1-\frac{\varepsilon}{4}, \quad 1+\frac{3\varepsilon}{4}\,.$$

To this order, the eigenvectors are independent of ε and given by

$$V_1 = \begin{pmatrix} \frac{1}{\sqrt{3}} \\ \sqrt{\frac{2}{3}} \\ 0 \end{pmatrix}, \quad V_2 = \begin{pmatrix} \frac{1}{\sqrt{2}} \\ -\frac{1}{2} \\ -\frac{1}{2} \end{pmatrix}, \quad V_3 = \begin{pmatrix} \frac{1}{\sqrt{6}} \\ -\frac{1}{2\sqrt{3}} \\ \frac{\sqrt{3}}{2} \end{pmatrix} \tag{21}$$

so that the mixing expected in this type of texture does not depend on ε, as long as it is non-zero. The vectors (21) are also eigenvectors of the unrenormalised texture (with $\varepsilon = 0$).

[2] For an alternative approach to the problem and a detailed discussion of fixed points for neutrino mixing angles, see also [23].

Let us now go back to the unperturbed texture. Since the latter has two exactly degenerate eigenvalues, there is arbitrariness in the choice of eigenvectors: the vectors corresponding to the two degenerate eigenvalues are not linearly independent, and can be rotated to different linear combinations, which still obey the orthogonality conditions. One example is the choice

$$\begin{aligned} V_1 &= \frac{1}{\sqrt{3}} V_1' + \sqrt{\frac{2}{3}} V_3' \,, \\ V_3 &= \frac{1}{\sqrt{3}} V_3' - \sqrt{\frac{2}{3}} V_1' \,, \end{aligned}$$

which gives

$$V_1' = \begin{pmatrix} 0 \\ \frac{1}{\sqrt{2}} \\ -\frac{1}{\sqrt{2}} \end{pmatrix}, \quad V_2' = \begin{pmatrix} \frac{1}{\sqrt{2}} \\ -\frac{1}{2} \\ -\frac{1}{2} \end{pmatrix}, \quad V_3' = \begin{pmatrix} \frac{1}{\sqrt{2}} \\ \frac{1}{2} \\ \frac{1}{2} \end{pmatrix} \tag{22}$$

corresponding to bimaximal mixing: $\phi_1 = \frac{\pi}{4}$, $\phi_2 = 0$ and $\phi_3 = \frac{\pi}{4}$. However, one cannot in general expect this latter combination of eigenvectors to be stable when the degenerate texture is perturbed, and the above analysis shows that, indeed, it is not. On the contrary, it is the direction given by (21) that is stable, and the absence of the parameter ε in the eigenvectors indicates that for this texture we may expect only minor modifications in the mixing, for $\tan\beta$ between 1 and 60.

4. Neutrino thresholds effects and Yukawa unification

From equations (7), we see that the Dirac neutrino Yukawa coupling,λ_N, will modify the ratio of λ_b/λ_τ (since the top Yukawa is close to a fixed point, the effects in it are relatively small). Using (7) we find that:

$$\lambda_b(t_N) = \rho \xi_t \frac{\gamma_D}{\gamma_E} \lambda_\tau(t_N), \quad \rho = \frac{\lambda_{b_0}}{\lambda_{\tau_0} \xi_N} \,. \tag{23}$$

For b–τ unification at $M_{\rm GUT}$, $\lambda_{\tau_0} = \lambda_{b_0}$. In the absence of the right-handed neutrino $\xi_N \equiv 1$, $\rho = 1$ and m_b at low energies is correctly predicted. In the presence of $\nu_{\rm R}$, however, $\lambda_{\tau_0} = \lambda_{b_0}$ at the GUT scale implies that $\rho \neq 1$ (since $\xi_N < 1$). To restore ρ to unity, a deviation from bottom–tau unification is required. For example, for $M_N \approx 10^{13}$ GeV and $\lambda_{t0} \geq 1$, it turns out that $\xi(t_N) \approx 0.89$. This corresponds to an approximate 10% deviation of the τ–b equality at the GUT scale, in agreement with the numerical results.

For large $\tan\beta$, even ignoring large corrections to m_b from superparticle loops [24,25] the effect of the heavy neutrino scale is much smaller, since now the bottom Yukawa coupling also runs to a fixed point [25] [3].

We can confirm these results by a numerical analysis, for neutrino parameters that are compatible with SuperKamiokande [27]. To do so, we choose a scale $M_{\rm GUT} \simeq 1.5 \times 10^{16}$ GeV, for which approximate unification of the three gauge couplings holds. We also choose a soft supersymmetry breaking scale of the order of 1 TeV, $\alpha_3(M_Z) \simeq 0.118$, $m_{\rm top} = 175$ GeV and $m_{\rm bot}^{\rm pole} = 4.8$ GeV. We then plot the ratio $m_\tau/m_b(M_{\rm GUT})$, as a function of M_N, for fixed values of $\tan\beta$. This is shown in Fig. 2, for a neutrino mass value $m_\nu = 0.03$ eV. In the figure, the lines are truncated when the value of M_N is such that the neutrino Yukawa coupling enters the non-perturbative regime.

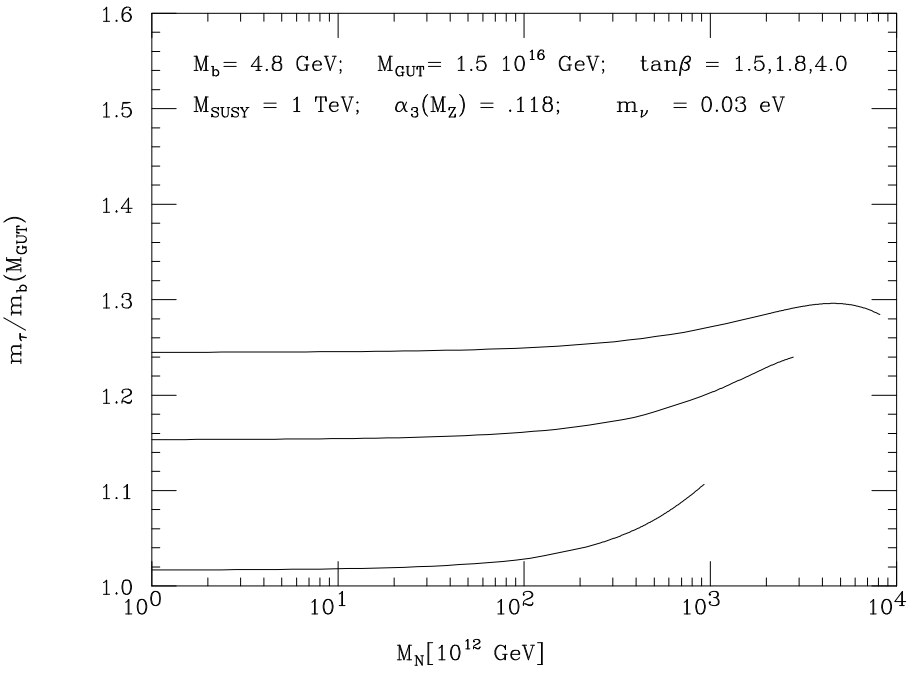

Fig. 2. The ratio $m_\tau/m_b(M_{\rm GUT})$ as a function of M_N, with the choice $m_\nu = 0.03$ eV and for different values of $\tan\beta$: from bottom to top, $\tan\beta = 1.5$, 1.8 and 4, respectively.

[3] For large $\tan\beta$, and $\lambda_b \approx \lambda_t$, the product and ratio of the top and bottom couplings can be simply expressed as $\lambda_t\lambda_b \approx \frac{8\pi^2\gamma_Q\,\gamma_D}{7\int\gamma_Q^2\,dt}$, $\frac{\lambda_t^2}{\lambda_b^2} \approx \frac{\gamma_Q^2}{\gamma_D^2}$ [26], indicating that one gets an approximate, model-independent prediction for both couplings at the low-energy scale.

We can then make the following observations:

(i) For small λ_N (small M_N in the see-saw model) the appearance of the neutrino masses does not play a major role. For small $\tan\beta$, in the region of the top infrared fixed-point, we obtain b–τ unification; when $\tan\beta$ increases, the expected deviation from b–τ unification is seen.

(ii) As λ_N becomes larger for fixed $\tan\beta$ (large M_N), the neutrino coupling lowers λ_τ with respect to λ_b; thus, to obtain the correct value of m_b/m_τ at low energies, we need to start with lower $\lambda_b/\lambda_\tau(M_{\rm GUT})$.

(iii) As λ_N increases, M_N gets close to the GUT scale and $\ln(M_N/M_{\rm GUT})$ decreases the magnitude of the effects. This explains the presence of a peak for $\tan\beta = 4$. For the other values of $\tan\beta$ the Dirac neutrino coupling is so large that λ_N enters the non-perturbative regime before this peak is reached.

Given these results, it is natural to ask if models with b–τ equality and large neutrino coupling at $M_{\rm GUT}$ may be consistent with the required neutrino masses in the small $\tan\beta$ regime. To answer this, we need to remember that the b–τ equality at the GUT scale refers to the $(3,3)$ entries of the charged lepton and down quark mass matrices, while the detailed structure of the mass matrices is not predicted by the grand unified group itself. It is then possible to assume mass textures, such that, after the diagonalisation at the GUT scale, the $(m_\ell^{\rm diag})_{33}$ and $(m_{\rm down}^{\rm diag})_{33}$ entries are no-longer equal [16].

To understand the effect, we consider a 2×2 example, and assume that the off-diagonal terms in the down-quark mass matrix $m_{\rm down}$ are small compared to the (33) element, whereas this is not the case for the charged-lepton mass matrix. In this case, one can approximate the down-quark and charged-lepton mass matrices at the GUT scale by

$$m^0_{\rm down} = A\begin{pmatrix} c & 0 \\ 0 & 1 \end{pmatrix}, \quad m^0_\ell = A\begin{pmatrix} x^2 & x \\ x & 1 \end{pmatrix}, \tag{24}$$

where A may be identified with $m_b(M_{\rm GUT})$, the bottom quark mass at the scale $M_{\rm GUT}$. At low energies, the eigenmasses are obtained by diagonalising the renormalized Yukawa matrices; this is equivalent to diagonalising the quark and charged-lepton Yukawa matrices at the GUT scale, and then evolving the eigenstates and the mixing angles separately. In this way, we see that the trace of the charged-lepton mass matrix, which gives the higher eigenvalue, is not 1 but $1+x^2$, and therefore the effective λ_b and λ_τ are not equal after diagonalization.

To restore b–τ unification in the cases with large deviation, large mixing in the charged lepton sector has to be introduced (parametrised by the factor x). Then the mixing in the neutrino sector, parametrised by an analogous factor y is also calculable. They both appear on the Tables II and III respectively, indicating that Yukawa unification can be a useful independent probe of neutrino and charged lepton textures.

TABLE II

Values of charged lepton μ–τ mixing leading to b–τ Yukawa coupling unification for $m_\nu = 0.03$ eV, for different choices of $\tan\beta$ and M_N.

$M_N[10^{13}$ GeV]	1	10	20	50	70	150	250	400
$\tan\beta = 1.5$	0.13	0.15	0.17	0.21	0.23			
$\tan\beta = 1.8$	0.39	0.40	0.40	0.41	0.42	0.43	0.44	
$\tan\beta = 4.0$	0.50	0.50	0.50	0.50	0.50	0.51	0.52	0.52

TABLE III

Values neutrino μ–τ mixing leading to b–τ Yukawa coupling unification for $m_\nu = 0.03$ eV, for different choices of $\tan\beta$ and M_N.

$M_N[10^{13}$ GeV]	1	10	20	50	70	150	250	400
$\tan\beta = 1.5$	-0.77	-0.73	-0.69	-0.62	-0.58			
$\tan\beta = 1.8$	-0.44	-0.43	-0.42	-0.40	-0.39	-0.37	-0.35	
$\tan\beta = 4.0$	-0.34	-0.33	-0.33	-0.32	-0.32	-0.31	-0.30	-0.29

5. Lepton flavour violating rare processes

In the Standard Model (SM) with massive neutrinos, $\mu \to e\gamma$ is mediated by diagrams of the type:

The decay rate for these processes is proportional to the neutrino mass square difference, scaling as $\Gamma \propto \frac{(m_2^2 - m_1^2)}{m_W^2} \sin^2\theta \cos^2\theta$. For δm_{12}^2 in the range indicated by the neutrino data, the branching ratio for this decay is $\leq 10^{-50}$, and thus too small to observe. The same is true for the rest of the flavour-violating processes.

However the situation is vastly different in supersymmetry, where in the presence of $\tilde{\mu}$-$\tilde{e}$ ($\tilde{\nu}_\mu$-$\tilde{\nu}_e$) mixing, one can generate the diagrams:

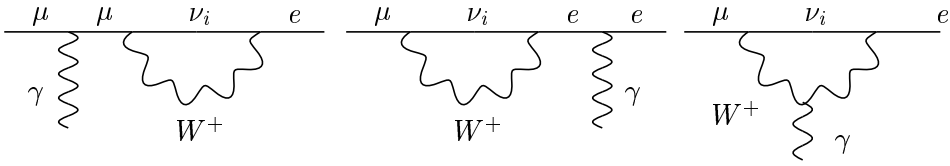

Fig. 3. Minimal Standard Model plus massive neutrino contributions to $\mu \to e\gamma$

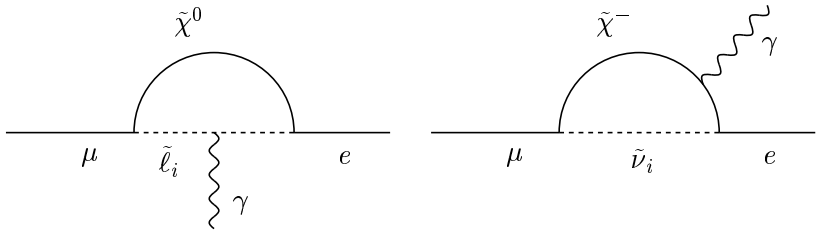

Fig. 4. Supersymmetric contributions to $\mu \to e\gamma$

Since the fermion in the loop is now a neutralino/chargino instead of a neutrino as in the previous case (with $m_{\tilde{\chi}^0}, m_{\tilde{\chi}^\pm} \gg m_\nu$), much larger rates are expected. The magnitude of the rates depends on the masses and mixings of superparticles. For non-universality at $M_{\rm GUT}$, large rates are in general expected. However, even if at $M_{\rm GUT}$

$$m_{\tilde{\ell},\tilde{\nu}} \propto \begin{pmatrix} 1 & 0 & 0 \\ 0 & 1 & 0 \\ 0 & 0 & 1 \end{pmatrix}$$

renormalisation group effects of the Minimal Supersymmetric Standard Model (MSSM) with right-handed neutrinos will spoil this diagonal form to give

$$m_{\tilde{\ell},\tilde{\nu}} \propto \begin{pmatrix} 1 & \star & \star \\ \star & 1 & \star \\ \star & \star & 1 \end{pmatrix} .$$

Indeed, the Dirac neutrino and charged lepton Yukawa couplings cannot, in general, be diagonalized simultaneously and since both these sets of lepton Yukawa couplings appear in the renormalisation-group equations, neither the lepton Yukawa matrices and the slepton mass matrices can not be simultaneously diagonalized at low energies either. Indeed, in the basis where m_ℓ is diagonal, the slepton-mass matrix acquires non-diagonal contributions

from renormalization at scales below $M_{\rm GUT}$, of the form [7]:

$$\delta\tilde{m}_\ell^2 \propto \frac{1}{16\pi^2}(3+a^2)\ln\frac{M_{\rm GUT}}{M_N}\lambda_N^\dagger\lambda_N m_{3/2}^2\,, \tag{25}$$

where a is related to the trilinear mass parameter, $A_\ell = am_{3/2}$, $m_{3/2}^2$ being the common value of the scalar masses at the GUT scale.

We stress that the effects of massive neutrinos are significant for models with universal scalar masses at the GUT scale, such as no-scale [28] and gauge-mediated models [29]. In models with non-universality at the GUT scale, excessive rates are generically predicted. In particular for models with universality at $M_{\rm GUT}$, different predictions for the various solutions of the solar neutrino deficit [30,31] (with a small/large mixing angle and with eV or ≈ 0.03 eV neutrinos), predict in general different rates for lepton flavour violation: the larger the μ–e mixing and the larger the neutrino mass scales that are required, the larger the rates. This already indicates that for degenerate neutrinos with bimaximal mixing, we expect significantly larger effects than for instance for hierarchical neutrinos with a small vacuum mixing angle. Note however that, for the just-so solutions to the solar neutrino problem, where a $\delta m^2 \approx 10^{-10}$ eV^2 is required, in the case of hierarchical neutrinos the predicted rates are small, even if the (1–2) mixing is large.

In order to estimate the expected effects, we look at a simple scheme based on abelian flavour symmetries and symmetric mass matrices [32]. For instance, for the charged-lepton matrix with a large (2–3) mixing in this model [33]

$$M_\ell \propto \begin{pmatrix} \overline{\varepsilon}^7 & \overline{\varepsilon}^3 & \overline{\varepsilon}^{7/2} \\ \overline{\varepsilon}^3 & \overline{\varepsilon} & \overline{\varepsilon}^{1/2} \\ \overline{\varepsilon}^{7/2} & \overline{\varepsilon}^{1/2} & 1 \end{pmatrix}\,, \qquad m_\nu^D \propto \begin{pmatrix} \varepsilon^7 & \varepsilon^3 & \varepsilon^{7/2} \\ \varepsilon^3 & \varepsilon & \varepsilon^{1/2} \\ \varepsilon^{7/2} & \varepsilon^{1/2} & 1 \end{pmatrix}\,, \tag{26}$$

$$V_\ell = \begin{pmatrix} 1 & \overline{\varepsilon}^2 & -\overline{\varepsilon}^{7/2} \\ -\overline{\varepsilon}^2 & 1 & \overline{\varepsilon}^{1/2} \\ \overline{\varepsilon}^{7/2} & -\overline{\varepsilon}^{1/2} & 1 \end{pmatrix}\,, \qquad V_{\nu_D} = \begin{pmatrix} 1 & \overline{\varepsilon}^4 & -\overline{\varepsilon}^7 \\ -\overline{\varepsilon}^4 & 1 & \overline{\varepsilon} \\ \overline{\varepsilon}^7 & -\overline{\varepsilon} & 1 \end{pmatrix} \tag{27}$$

a small μ–e mixing is always predicted, as a result of fixing the charged lepton hierarchies.

In this model, we calculated the rates for $\mu \to e\gamma$ and μ–e conversion, which are experimentally most promising. The rates depend on supersymmetric masses and mixings; we parametrize the supersymmetric masses in terms of the universal GUT-scale parameters m_0 and $m_{1/2}$, and use the renormalization-group equations of the MSSM to calculate the low-energy

sparticle masses. Other relevant free parameters of the MSSM are the trilinear coupling A, the sign of the Higgs mixing parameter μ, and the value of $\tan\beta$. Here we fix the value of $A_0 = -m_{1/2}$ and assume the sign of the μ parameter to be either positive or negative. Contour plots for $\mu \to e\gamma$ appear in Fig. 5.

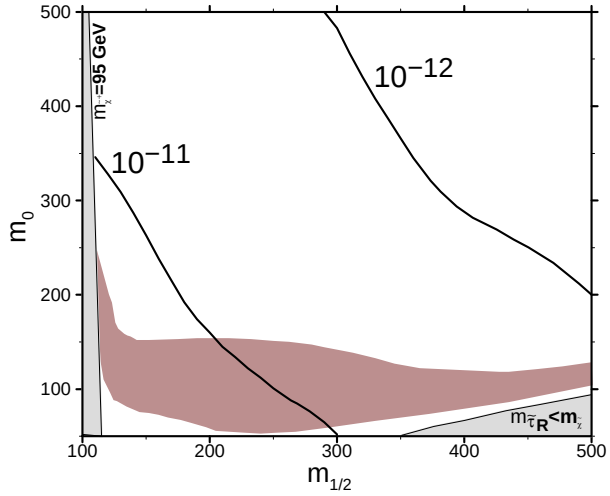

Fig. 5. Contour plot in the $(m_{1/2}, m_0)$ plane for the decays $\mu \to e\gamma$, assuming $\tan\beta = 3$ and $\mu < 0$. The rates are encouraging throughout the dark-shaded region preferred by astrophysics and cosmology [35].

We observe that, as expected, the branching ratios tend to decrease as $m_{1/2}$ and m_0 increase. For $\tan\beta = 3$, as chosen in the contour plot, we predict values of $\mathrm{BR}(\mu \to e\gamma)$ compatible with the experimental bound in most of the region where the cosmological relic density is in the range preferred by astrophysics (dark shaded-region in plot). In contrast, if $\tan\beta \geq 10$, acceptable $\mathrm{BR}(\mu \to e\gamma)$ rates are found only for large values of $m_0 \geq 400$ GeV. The light-shaded areas in Fig. 5 correspond to the regions of the $(m_{1/2}, m_0)$ plane that are excluded by LEP searches for charginos and by the requirement that the lightest supersymmetric particle not be charged [35].

Let us now briefly discuss the rare processes $\mu \to 3e$ and $\mu \to e$ conversion on nuclei. These decays receive contributions from three types of Feynman diagrams. The first are photon 'penguin' diagrams related to the diagrams for $\mu \to e\gamma$ discussed above, where now the photon is virtual and couples to an e^+e^- (or quark-antiquark) pair. A second class of diagrams is obtained by replacing the photon line with a Z boson. Finally, there are also box diagrams. In addition, all the above types of diagrams are accompa-

nied by their supersymmetric analogues. We have evaluate all the relevant diagrams exactly in the numerical analysis, but one has approximately the relations (restricting himself to the photonic contribution which dominates over a large portion of the parameter space)

$$\frac{\Gamma(\mu^+ \to e^+e^+e^-)}{\Gamma(\mu^+ \to e^+\gamma)} \approx 6 \times 10^{-3}\,, \tag{28}$$

and

$$\mathrm{R}(\mu Ti \to eTi) \approx 5.6 \times 10^{-3}\mathrm{BR}(\mu \to e\gamma)\,. \tag{29}$$

Among these two processes, $\mu \to e$ conversion is the most interesting since with an intense proton (and muon) source, such as that projected for a neutrino factory or a muon collider, experiments sensitive to rates as low as 10^{-16} may be feasible [14].

Fig. 6 displays contours of the rate for $\mu \to e$ conversion in the $(m_0, m_{1/2})$ plane. We see that the former predicts a rather larger rate, which offers good prospects for observation throughout the region preferred by cosmology, in the next generation of experiments, even for neutrino textures with hierarchical neutrinos and μ–e mixing in the small MSW region for the solar neutrino deficit.

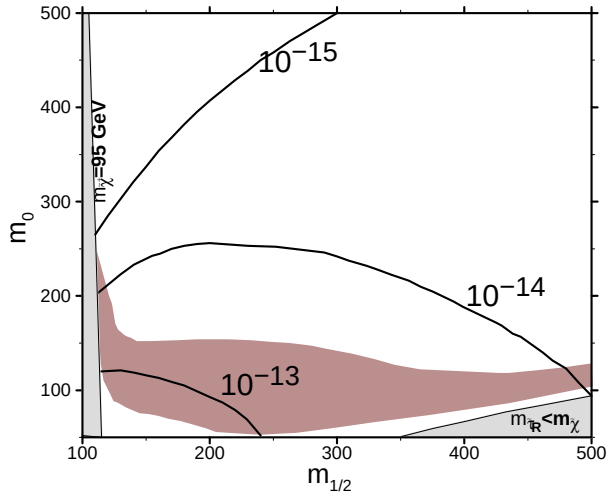

Fig. 6. Contour plots in the $(m_{1/2}, m_0)$ plane for $\mu \to e$ conversion, assuming $\tan\beta = 3$ and $\mu < 0$. We see that the conversion rate is encouraging throughout the dark-shaded region preferred by astrophysics and cosmology [35].

6. Conclusions

We discussed various aspects of the renormalisation-group effects of neutrino masses and interactions. In supersymmetric extensions of the Standard Model, these effects are important. In particular, for small $\tan\beta$, b–τ unification requires the presence of significant μ–τ flavour mixing. On the other hand, for large $\tan\beta$, small mixing at the GUT scale may be amplified to maximal mixing at low energies, and *vice versa*. The eigenvalues of the neutrino mass operator are also modified by quantum corrections; given the very small mass differences required to address the solar and atmospheric neutrino deficits, several neutrino textures (especially those generating degenerate neutrinos can be constrained or in certain models, even excluded). Finally, while in the minimal scheme with SM plus neutrino masses the rates for rare muon decays and μ–e conversion in nuclei are very suppressed, this is no longer the case in supersymmetric models. In this latter case, even for universality of soft terms at the GUT scale, renormalisation group corrections due to lepton mixing induce rates that are very close to the current experimental bounds and within probe in the next generation of experiments.

REFERENCES

[1] Y. Fukuda *et al.*, SuperKamiokande collaboration, *Phys. Lett.* **B433**, 9 (1998); *Phys. Lett.* B436 (1998) 33; *Phys. Rev. Lett.* **81**, 1562 (1998).

[2] M. Apollonio *et al.*, Chooz collaboration, *Phys. Lett.* **B420**, 397 (1998).

[3] See for example, L. Wolfenstein, *Phys. Rev.* **D17**, 20 (1978); S.P. Mikheyev, A.Yu. Smirnov, *Yad. Fiz.* **42**, 1441 (1985) and *Sov. J. Nucl. Phys.* **42**, 913 (1986).

[4] M. Gell-Mann, P. Ramond, R. Slansky, *Proceedings of the Stony Brook Supergravity Workshop*, New York 1979, eds. P. Van Nieuwenhuizen, D. Freedman, North-Holland, Amsterdam.

[5] Z. Maki, M. Nakagawa, S. Sakata, *Prog. Theor. Phys.* **28**, 247 (1962).

[6] S.T. Petcov *Yad. Phys.* **25**, 641 (1977) and *Sov. J. Nucl. Phys.* **25**, 340 (1977); S.M. Bilenki, S.T. Petcov, B. Pontecorvo, *Phys. Lett.* **B67**, 309 (1977).

[7] F. Borzumati, A. Masiero, *Phys. Rev. Lett.* **57**, 961 (1986); J. Ellis, D.V. Nanopoulos, *Phys. Lett.* **B110**, 44 (1982); R. Barbieri, R. Gatto, *Phys. Lett.* **B110**, 211 (1982); L.J. Hall, V.A. Kostelecky, S. Raby, *Nucl. Phys.* **B267**, 415 (1986); G.K. Leontaris, K. Tamvakis, J.D. Vergados, *Phys. Lett.* **B171**, 412 (1986); J. Hisano, T. Moroi, K. Tobe, M. Yamaguchi, *Phys. Rev.* **D53**, 2442 (1996); S.F. King, M. Oliveira, *Phys. Rev.* **D60**, 035003 (1999).

[8] R. Barbieri *et al.*, *Nucl. Phys.* **B445**, 219 (1995); S. Dimopoulos, D. Sutter, *Nucl. Phys.* **B452**, 496 (1995); M.E. Gómez, H. Goldberg, *Phys. Rev.* **D53**, 5244 (1996); A. Ilakovac, A. Pilaftsis, *Nucl. Phys.* **B437**, 491 (1995); G.K. Leontaris, N.D. Tracas, *Phys. Lett.* **B431**, 90 (1998); M. Gómez, *et al.*, *Phys. Rev.* **D59**, 116009 (1999); J. Hisano, D. Nomura, *Phys. Rev.* **D59**, 116005 (1999); R. Kitano, K. Yamamoto, `hep-ph/9905459`; Y. Okada, K. Okumura, `hep-ph/9906446`; J.L. Feng, Y. Nir, Y. Shadmi, `hep-ph/9911370`.

[9] For a recent review, see: Y. Kuno, Y. Okada, `hep-ph/9909265`.

[10] M.L. Brooks *et al.*, MEGA collaboration, `hep-ex/9905013`.

[11] U. Bellgardt *et al.*, *Nucl. Phys.* **B229**, 1 (1988).

[12] P. Wintz, Proceedings of the First International Symposium on Lepton and Baryon Number Violation, p. 534.

[13] S. Ahmed *et al.* , CLEO Collaboration, `hep-ex/9910060`.

[14] See, for example: W.J. Marciano, Workshop on Physics at the first Muon Collider and at the Front End of the Muon Collider; Prospective Study of Muon Storage Rings at CERN, eds. B. Autin, A. Blondel, J. Ellis, CERN Report 99-02 (1999).

[15] F. Vissani, A. Yu. Smirnov, *Phys. Lett.* **B341**, 173 (1994); A. Brignole, H. Murayama, R. Rattazzi, *Phys. Lett.* **B335**, 345 (1994).

[16] G.K. Leontaris, S. Lola, G.G. Ross, *Nucl. Phys.* **B454**, 25 (1995); S. Lola, `hep-ph/9903203`, Proceedings of the 1998 Corfu Summer Institute on Elementary Particle Physics, published in JHEP.

[17] See for instance the last two papers in [7] and references therein.

[18] K. Babu, C.N. Leung, J. Pantaleone, *Phys. Lett.* **B319**, 191 (1993); P.H. Chankowski, Z. Pluciennik, *Phys. Lett.* **B316**, 312 (1993); M. Tanimoto, *Phys. Lett.* **B360**, 41 (1995); N. Haba, Y. Matsui, N. Okamura, M. Sigiura, *Eur. Phys. J.* **C10**, 677 (1999) and `hep-ph/9908429`.

[19] J. Ellis *et al.*, *Eur. Phys. J.* **C9**, 389 (1999).

[20] J. Ellis, S. Lola, *Phys. Lett.* **B458**, 310 (1999).

[21] R. Barbieri, G.G. Ross, A. Strumia, *JHEP* **020**, 9910 (1999).

[22] A. Casas, J.R. Espinosa, A. Ibarra, I. Navarro, *Nucl. Phys.* **B556**, 3 (1999); *JHEP* **015**, 9909 (1999); `hep-ph/9905381`; `hep-ph/991042`.

[23] P.H. Chankowski, W. Krolikowski, S. Pokorski, *Phys. Lett.* **B473**, 109 (2000); S. Pokorski, talk at the Cracow Epiphany Conference, 2000.

[24] L. Hall *et al.*, *Phys. Rev.* **D50**, 7048 (1994);

[25] M. Carena *et al.*, *Nucl. Phys.* **B426**, 269 (1994).

[26] E.G. Floratos, G.K. Leontaris, S. Lola, *Phys. Lett.* **B365**, 149 (1996).

[27] M. Carena, J. Ellis, S. Lola, C.E.M. Wagner, `hep-ph/9906362`, to appear in the *Eur. Phys. J.* **C**.

[28] J. Ellis, C. Kounnas, D.V. Nanopoulos, *Nucl. Phys.* **B247**, 373 (1984); J. Ellis, *et al.*, *Phys. Lett.* **B134**, 429 (1984).

[29] M. Dine, A. Nelson, *Phys. Rev.* **D48**, 1277 (1993); M. Dine, *et al.*, *Phys. Rev.* **D53**, 2658 (1996); S. Dimopoulos, S. Thomas, J.D. Wells, *Nucl. Phys.* **B488**, 39 (1997); G. Giudice, R. Rattazzi, `hep-ph/9801271`, and references therein.

[30] V. Barger, S. Pakvasa, T.J. Weiler, K. Whisnant, *Phys. Lett.* **B437**, 107 (1998); A.J. Baltz, A.S. Goldhaber, M. Goldhaber, *Phys. Rev. Lett.* **81**, 5730 (1998). See also: R. N. Mohapatra, S. Nussinov, *Phys. Lett.* **B441**, 299 (1998), `hep-ph/9809415`; C. Jarlskog, M. Matsuda, S. Skadhauge, `hep-ph/9812282`; Y. Nomura, T. Yanagida, *Phys. Rev.* **D59**, 017303 (1999); S.K. Kang, C.S. Kim, *Phys. Rev.* **D59**, 091302 (1999); H. Georgi, S.L. Glashow, `hep-ph/9808293`; Y. L. Wu, *Phys. Rev.* **D59**, 113008 (1999); *Eur. Phys. J.* **C10**, 491 (1999); *Int. J. Mod. Phys.* **A14**, 4313 (1999); C. Wetterich, *Phys. Lett.* **B451**, 397 (1999); R. Barbieri, L.J. Hall, G.L. Kane, G.G. Ross, `hep-ph/9901228`.

[31] Some of the many references are: C. Wetterich, *Nucl. Phys.* **B261**, 461 (1985); G.K. Leontaris, D.V. Nanopoulos, *Phys. Lett.* **B212**, 327 (1988); Y.Achiman, T. Greiner, *Phys. Lett.* **B329**, 33 (1994); H. Dreiner *et al.*, *Nucl. Phys.* **B436**, 461 (1995). Y. Grossman, Y. Nir, *Nucl. Phys.* **B448**, 30 (1995); P. Binétruy, S. Lavignac, P. Ramond, *Nucl. Phys.* **B477**, 353 (1996); G.K. Leontaris, S. Lola, C. Scheich, J.D. Vergados, *Phys. Rev.* **D53**, 6381 (1996); S. Lola, J.D. Vergados, *Prog. Part. Nucl. Phys.* **40**, 71 (1998); B.C. Allanach, `hep-ph/9806294`; P. Binétruy *et al.*, *Nucl. Phys.* **B496**, 3 (1997); G. Altarelli, F. Feruglio, *Phys. Lett.* **B439**, 112 (1998); *JHEP* **021**, 9811 (1998); *Phys. Lett.* **B451**, 388 (1999) and `hep-ph/9905536`; G. Altarelli, F. Feruglio, I. Masina, `hep-ph/9907532`; Y. Nir, Y. Shadmi, *JHEP* **023**, 9905 (1999).

[32] L. Ibanez, G.G. Ross, *Phys. Lett.* **B332**, 100 (1994).

[33] S. Lola, G.G. Ross, *Nucl. Phys.* **B553**, 81 (1999).

[34] J. Ellis, M.E. Gomez, G.K. Leontaris, S. Lola, D.V. Nanopoulos, `hep-ph/9911459`, to appear in *Eur. Phys. J.* **C**.

[35] J. Ellis, T. Falk, K.A. Olive, *Phys. Lett.* **B444**, 367 (1998).